NACA TN 4205

NATIONAL ADVISORY COMMITTEE FOR AERONAUTICS

TECHNICAL NOTE 4205

TRANSIENT HEATING EFFECTS ON THE BENDING STRENGTH OF INTEGRAL ALUMINUM-ALLOY BOX BEAMS

By Richard A. Pride and John B. Hall, Jr.

Langley Aeronautical Laboratory
Langley Field, Va.

Washington
March 1958

1Y

NATIONAL ADVISORY COMMITTEE FOR AERONAUTICS

TECHNICAL NOTE 4205

TRANSIENT HEATING EFFECTS ON THE BENDING STRENGTH OF INTEGRAL ALUMINUM-ALLOY BOX BEAMS

By Richard A. Pride and John B. Hall, Jr.

SUMMARY

Twenty-five square-tube beams made of aluminum alloy were tested to failure under various combinations of bending moment and transient heating. Two types of heat input were used so that the effect of thermal stresses could be separated from effects of material properties. Two sizes of square tubes were tested so that both elastic and plastic buckling stresses would be obtained.

Good agreement was found between the buckling loads determined experimentally for both types of heat input and local buckling loads calculated according to a theory that incorporates the effects of material properties and thermal stress in both the elastic- and the plastic-stress ranges. A marked reduction in buckling strength was observed as a result of thermal stress.

Failure of the compression side of the beam occurred in all tests. The maximum loads when plotted as a function of temperature appeared as a single scatter band for both types of heat inputs and correlated well with the loads calculated by a maximum-strength theory based solely on material properties without consideration of thermal stresses. These results indicate that thermal stresses which influence the magnitude of the buckling load are largely alleviated in the interval between local buckling and maximum load.

This limited study indicates that both local buckling and maximum bending strength appear to be essentially independent of the sequence of loading and heating.

INTRODUCTION

The short-time static strength of composite structures, such as multiweb box beams, can generally be calculated satisfactorily at constant elevated temperatures. Equations for predicting both buckling and maximum strength at room temperature can be adapted to elevated

temperatures by using material properties obtained from stress-strain curves for the appropriate temperature and exposure time. However, under transient heating, thermal stresses usually develop so that steady-state methods for predicting buckling and maximum strength may require modification in order to combine the effects of thermal stress and load stress in both the elastic- and the plastic-stress ranges. To date, most of the theoretical treatments for predicting combined thermal and load stresses have dealt with elastic conditions and only a few have considered nonlinear combinations of either elastic or plastic stresses. An approximate method for combining thermal and load stresses which produce buckling in box beams was given in reference 1 with two verifying tests, and further substantiation was obtained experimentally in reference 2.

The purpose of the present investigation was to determine the interaction effects of external loading and rapid nonuniform or uniform heating on both buckling and the compressive failure of box beams. Nonuniform heating can produce large thermal stresses, whereas uniform heating generally produces negligible thermal stresses. In the present investigation the test specimens were integral square tubes and represented an idealization of the load-carrying portion of an airplane or missile wing. Equations for buckling and maximum bending strength are derived and the calculated results are compared with the experimental data.

Some of the material presented herein was originally included in a thesis submitted to the Virginia Polytechnic Institute by Richard A. Pride in partial fulfillment of the requirements for a Master of Science Degree in Applied Mechanics.

SYMBOLS

A	cross-sectional area, sq in.
b	plate width, in.
c	distance from neutral axis of beam to center of skin, in.
E	Young's modulus, ksi
E_S	secant modulus for skin, ksi
E_W	secant modulus for web, ksi
I	moment of inertia, $in.^4$
k	plate buckling coefficient

M	bending moment, in-kips
T	temperature, $^{\circ}F$
$\overline{T}$	average temperature, $^{\circ}F$
t	plate thickness, in.
α	coefficient of thermal expansion, per $^{\circ}F$
ϵ	strain associated with stress
ϵ_t	total strain associated with stress and thermal expansion
η	plasticity reduction factor
μ	Poisson's ratio
σ	stress, ksi

Subscripts:

B	bending
cr	critical
cy	0.2-percent-offset compressive yield
f	failure
o	initial
S	skin
W	web

EXPERIMENTAL INVESTIGATION

The test specimens used in the present investigation consisted of 25 drawn square tubes, 8 feet long, of 2014-T6 aluminum alloy. Twelve of the specimens were 5.00 inches square with a wall thickness of 0.154 inch and 13 specimens were 7.50 inches square with a wall thickness of 0.152 inch. These beam specimens were selected so that the 5.00-inch-square tubes would buckle at a stress slightly greater than the proportional limit of the material when the beams were subjected to a pure

bending moment at room temperature, whereas the larger beams were chosen so that they would buckle at less than one-half the proportional limit stress.

Each beam was tested in such a manner that a pure bending moment was applied over the central 28 inches of the beam, with or without the presence of external heating. (See fig. 1.) Two tests, one for each size beam, were made without heating; in these tests, the moment was increased until buckling and then failure occurred. In the other tests, 13 of the beams were heated rapidly to a predetermined temperature level and then loaded to buckling and failure, and 10 of the beams were loaded to a predetermined bending moment and then heated rapidly until buckling and then failure occurred.

Two kinds of heat input were used for the 23 tests involving external heating. In 14 tests the tension and compression skins of the beams were heated at a rate of approximately 50 Btu/(sec)(sq ft) (equivalent to a temperature rise of 100° F per second) while the webs were shielded from heating in order to produce large thermal stresses; hereafter, this type of heating is referred to as skin heating. In 9 tests all four sides of the beams were heated so that negligible thermal stresses resulted; hereafter, this type of heating is referred to as uniform heating. Temperatures were measured by iron-constantan thermocouples, strains in the unheated webs were measured by Baldwin SR-4 type A-9 wire strain gages, and deflections were measured with linear variable differential transformer gages. Strain and deflection records were used to determine when buckling occurred in the tests in which skin heating was used, but only deflection records could be used in the tests in which uniform heating was used because strain gages were not attached. Additional instrumentation details are given in appendix A.

Tensile tests were performed under constant load with rapid heating on material coupons to obtain information on material properties for use in evaluation of the beam tests. The details on material properties are discussed in appendix B.

RESULTS AND DISCUSSION

Temperature Distributions

Prior to the tests with combined heating and loading, a preliminary investigation was made to determine the temperature distribution resulting from both skin heating and uniform heating. Results typical of these tests are partially illustrated in figure 2 which shows that longitudinally the temperatures dropped off considerably near the ends of the test section but that the temperatures were nearly uniform in the central third

of this section. Hence buckling and failure could be expected to occur in this central region; therefore, further discussion of temperature effects, such as the cross-sectional temperature distributions produced by both types of heating, is restricted to this area.

For the skin heated beams, typical cross-sectional temperature results are shown in figure 3 for the 5.00-inch-square tubes and in figure 4 for the 7.50-inch-square tubes. The temperatures in only one quadrant are shown because similar results were obtained for the other quadrants. Because of the side reflectors used in these tests, a fairly uniform heating was applied to the skins; consequently, the drop in temperature in the skin near the web junction indicates primarily the effects of conduction into the heat sink afforded by the unheated web. The temperature distributions shown (figs. 3 and 4), wherein a portion of the skin has been heated to slightly above 500° F and part of the web has remained at a temperature of less than 100° F, result in peak thermal stresses of about 30 ksi in the central portion of both the skins and webs. The approximated average temperatures for the skin and web, illustrated by the dashed lines in figures 3 and 4, were determined as explained in appendix C.

For the uniformly heated beams, typical cross-sectional temperature results for the 5.00- and 7.50-inch-square-tube beams are shown in figures 5 and 6, respectively. The average temperatures, indicated by the dashed lines, were obtained by averaging all available temperatures. (See appendix C.) Deviations from average temperatures were ±6 percent of average temperature for the 5.00-inch-square tubes and ±10 percent for the 7.50-inch-square tubes.

Buckling

A comparison between the experimental and calculated external moments required to produce local buckling for both uniformly heated and skin heated beams is shown in figure 7. The experimental bending moment which produced local buckling is plotted against the average skin temperature for the 5.00-inch-square tubes in figure 7(a) and for the 7.50-inch-square tubes in figure 7(b). The experimental buckling moments and temperatures are given in table I, and the method used for the determination of experimental buckling from the strain and deflection records is discussed in appendix C. The buckling-moment curves shown in figure 7 for both uniformly heated and skin heated beams were obtained by calculating a buckling stress for the skin, by means of relations which are defined subsequently, and then substituting this buckling stress into the elementary beam-bending formula $M = \frac{\sigma I}{c}$.

The moment calculated in this manner is rigorous for elastic buckling, such as occurred, for example, in the 7.50-inch-square tubes. For the 5.00-inch-square tubes the buckling stress for the cover was predicted to be in the plastic-stress range, and use of this expression to determine buckling moment gives conservative results because a linear stress distribution is assumed in the webs. The magnitude of the plastic strain developed in the 5.00-inch-square tubes at buckling was small, and the use of the elementary beam formula is therefore considered to be satisfactory in this case.

For uniform heating, the skin buckling stress was predicted from the following plate-buckling equation:

$$\sigma_{cr} = \frac{-k\pi^2\eta E}{12\left(1 - \mu^2\right)}\left(\frac{t}{b}\right)^2 \tag{1}$$

where $\eta = 1$ in the elastic-stress range and $\eta = \frac{E_S}{E}$ in the plastic-stress range. Compression stress was taken as negative, and the value of k was taken to be 5.32. (See appendix C.) The predicted buckling moments obtained with the buckling stress calculated from equation (1) are shown in figure 7 to be in satisfactory agreement with the test results except for two test points shown in figure 7(b) (beams 14 and 18 in table I) which are higher than the calculated buckling moments. Some of this disagreement between experimental and calculated results may be attributed to the difficulty experienced in estimating the experimental buckling moment from the test records as described in appendix C.

For symmetrical skin heating, the magnitude of the load stress that can be superimposed on the thermal stress to produce buckling of the compression skin is given by the following equation:

$$\sigma_B = \sigma_{cr} + \frac{\alpha E_S\left(\overline{T}_S - \overline{T}_W\right)}{1 + \frac{E_S A_S}{E_W A_W}} \tag{2}$$

where σ_{cr} is the buckling stress given by equation (1) and the last term (see appendix C) defines the thermal stress in the skin. Equation (2) is applicable in either the elastic- or plastic-stress ranges. In deriving equation (2), α was assumed to vary linearly from 12.5×10^{-6}

at 80° F to 13.7×10^{-6} at 600° F. This variation of α with temperature is comparable to the values given in reference 3.

The lower curves in figures 7(a) and 7(b) were calculated by substituting σ_B from equation (2) into the moment expression. The predicted buckling moments are in satisfactory agreement with the results of the tests in which skin heating was used in both the elastic- and the plastic-stress ranges. No discernible effects of the sequence of loading and heating are evident.

It thus appears that the magnitude of the externally applied moment required to produce local buckling of beams with integral webs can be predicted at elevated temperatures in both the elastic- and plastic-stress ranges. The calculated buckling moment is in satisfactory agreement with test results for either uniform heating where no appreciable thermal stresses are developed or for skin heating where significant thermal stresses are produced.

Failure

The failure moments and temperatures given in table I were experimentally determined from the test records at the instant when an abrupt increase in beam deflection occurred, followed by almost instantaneous collapse of the beam. Determination of failure was facilitated by the autographic recording of the output from the transformer deflection gages. (See appendix A.) Failures occurred in all the beams in the compression skin in a localized region near the center. Visual examination of the specimens after failure indicated that one buckle of a series of four or five in the compression skin developed excessive distortions and the beam was unable to sustain the applied load in the region of the excessively distorted buckle.

A comparison of the failure moments experimentally determined with those calculated is shown in figure 8. The lower curves in figures 8(a) and 8(b) are calculated failure moments for the uniformly heated beams. These curves were established from the following equation (for the derivation of this equation, see appendix C):

$$M_f = 1.84\sqrt{E_S\sigma_{cy}}t_S^2 b_W + 0.400\sigma_{cy}b_W^2 t_W \qquad (3)$$

The first term on the right-hand side of this equation defines the moment carried by the compression skin and the last term, the moment carried by the webs. In this last term a partially plastic stress distribution for the web is assumed. The lower curves are in good agreement with the test

results for the uniformly heated beams in figure 8(a), and they are in only fair agreement with the test results for the uniformly heated beams in figure 8(b).

The upper curves in figures 8(a) and 8(b) for the tests in which skin heating was used were also obtained from equation (3) by using material properties corresponding to the average temperature of the heated skin in the first term on the right-hand side of the equation and properties corresponding to the average temperature of the unheated webs in the last term. These calculations give a somewhat higher failure moment than would be obtained if the moment carried by the webs were determined by taking incremental areas of the web and determining the moment for each incremental area at its appropriate temperature. These calculations of failure moment for skin heating neglect the presence of thermal stresses at maximum load. Since the predicted moments are in satisfactory agreement with the experimental results, it appears that thermal stresses were almost entirely alleviated in the interval between local buckling and failure regardless of whether buckling occurred in the elastic- or the plastic-stress range of the material.

Note that the test results for the failure moment for both uniformly and skin heated beams appear as a single scatter band in figure 8 in contrast with the results obtained for buckling (fig. 7) which fall into two distinct groups. A slight effect of sequence of loading and heating on failure can be noted for the 5.00-inch-square tubes in figure 8(a). The test points for specimens heated and then loaded appear to fall slightly below the corresponding test points for specimens loaded and then heated. A similar effect is not apparent for the 7.50-inch-square tubes in figure 8(b).

The results of this study indicate that the maximum strength of the beams can be predicted satisfactorily solely on the basis of material properties and without consideration of thermal stresses. Therefore, it appears reasonable to assume that similar results would be obtained for other heating rates and beam proportions. For lower heating rates or for beams which contain less web material with respect to the cover skins, smaller skin thermal stresses would be developed than were obtained in this study. Smaller thermal stresses would not be expected to influence the maximum bending strength. Heating rates higher than those used in the present study could produce less than a 15-percent increase in thermal stress for any given skin temperature because an infinite heating rate would produce only a 15 percent greater difference between the skin and web temperatures. This small increase in thermal stresses would again be expected to have only a negligible effect on the maximum bending strength of the beams.

CONCLUDING REMARKS

Twenty-five square-tube beams were tested under various combinations of bending load and symmetrical heating at skin temperature rates of about 100° F per second. Two types of radiant heat input were used; inputs which heated all four sides uniformly produced temperature without thermal stress, and inputs which heated only the compression and tension skins produced both temperature and thermal stress. Two sizes of square tubes were tested so that buckling stresses were elastic for one size and plastic for the other size.

Local buckling of the skin of these beams occurred in every test and the results are divided into two categories for each of the two beam proportions: buckling without appreciable thermal stress occurred with the buckling stress dependent only on the elevated-temperature properties of the material both in the elastic- and the plastic-stress ranges, and buckling under heating conditions that produced significant thermal stress occurred with the buckling stress dependent on the induced thermal stresses as well as on elevated-temperature properties of the material.

Good agreement was shown between the buckling loads experimentally determined and those calculated by a theory incorporating material properties and thermal stress in both the elastic- and the plastic-stress ranges.

Failure of the compression cover of the beams occurred in all tests. For both types of heat input, the maximum bending strength, when plotted against average skin temperature, appears as a single scatter band for each beam proportion. Maximum bending strength predicted solely on the basis of material properties showed good correlation with the test results; this correlation indicates that thermal stresses were largely alleviated in the interval between local buckling and failure.

The influence of sequence of loading and heating was practically negligible on buckling strength and small at failure for beams at the high plastic-stress level. Beams heated first and then loaded appeared to have slightly lower maximum bending strength than those loaded first and then heated.

Langley Aeronautical Laboratory,
National Advisory Committee for Aeronautics,
Langley Field, Va., December 5, 1957.

APPENDIX A

TEST SETUP AND INSTRUMENTATION

Test Setup

An overall view of the test setup is shown in figure 1. A four-point loading system was used to produce a pure bending moment in the center section of the specimen. Vertical loads were applied at the ends of the beam by 20-kip-capacity jacks which were actuated by a controlled air-pressure system. Loads could be increased continuously up to capacity or a given load could be applied and held constant throughout large displacements of the jacks. Constant load could be maintained by means of a large-volume air-storage reservoir. Under constant load conditions, change in pressure and load was less than 0.1 percent of indicated pressure for full-jack displacement.

Applied loads were measured by Baldwin SR-4 load cells inserted in the tensile linkage between the jacks and the ends of the beam (fig. 1). The applied pressure in the jacks was also measured by a strain-gage-type pressure pickup for a check on the applied load.

Heating of the specimen on the compression and tension skins, as shown in figure 1, or on all four sides in the pure bending test section was accomplished with quartz-tube lamp radiators. Each radiator used in this test setup heated one side of the beam and had approximately 10 by 24 inches of radiant surface. The heating rate of the specimen was increased by using alclad reflectors between the radiators and the corners of the beam cross section and by painting the surface with flat black lacquer. The heating rate was nominally the same in all tests and averaged about 50 Btu/(sec)(sq ft) on the specimen surface, which is equivalent to a skin temperature rate of 100° F per second.

Thermocouples

All thermocouples were made of No. 30 iron-constantan wire. After considerable experimentation the following procedure was adopted for use in the test. Two small holes (0.0210-inch diameter) were drilled through the square-tube wall thickness about 1/8 inch apart at the desired location of the thermocouple. Bare individual iron or constantan wires were inserted through the holes and extended out through the ends of the tubes. The ends of the wires were peened into the outer surface of the beams so as to make a double junction of iron to aluminum and aluminum to constantan. This type of installation in effect measured the average temperature

of the wall between the two holes. Each bare wire inside the tube was insulated with fiber glass sleeving.

This method of installation was selected because it avoided the possibility of poor physical contact sometimes encountered when a welded thermocouple bead is peened into a hole. The dual installation could be checked electrically for poor contact, whereas the usual single thermocouple bead would indicate electrical continuity even though the bead was completely free of the material. Good electrical contact in the dual installation indicated good heat-transfer characteristics between the thermocouple wires and the specimen. Installing the thermocouple wires inside the beams avoided direct exposure to the radiation and prevented overheating of the wires and subsequent errors in the indicated temperatures.

Deflection Pickups

Beam deflection records were used to determine when buckling and maximum strength were reached experimentally as discussed in appendix C. Deflection measurements were obtained along the center line of the beam by using steel rods which extended horizontally through the beam cross section and from which aluminum U-frames were suspended. (See fig. 1.) The cores of linear variable differential transformers were connected to the bottoms of the U-frames so that vertical motion of the beam at the point of suspension resulted in an equal amount of displacement of the transformer cores. Three deflection stations along the longitudinal center line were utilized in all tests: one at the center of the test section and one 6 and one 9 inches away from the center.

In order to minimize expansion of the U-frames when exposed to heat in the uniform heating case, the portion extending inside the radiation area was loosely wrapped with aluminum foil. As a check on indicated deflection resulting from expansion, a heating run was made without loading on a specimen of each size. For the sensitivity with which the deflection gages were operated on the 5.00-inch-square tubes, deflection indications were indiscernible during heating and for as long as 3 seconds after heating, which covered the time range of most of the tests. For the 7.50-inch-square tubes, smaller overall deflections were expected; therefore, a greater sensitivity was used. With this greater sensitivity, U-frame expansion from heating was measurable, and corrections had to be made to the individual test deflections based on peak temperature achieved and on elapsed time after heating.

Strain Gages

For the tests in which skin heating was used, strain records were used in addition to the beam deflection records to determine experimental buckling and maximum strength as discussed in appendix C. Baldwin SR-4 type A-9 wire strain gages were located in a longitudinal direction on the outside of the webs of the beams at sufficient distances from the heated skins to avoid excessive heating during a test. For the 5.00-inch-square tubes, gages were located on the web center line and 1 inch above and below the center line. For the 7.50-inch-square tubes, gages were located on the web center line and 2 inches above and below the center line. At these locations the maximum temperature rise experienced during a test was about 50° F.

Any temperature rise in the material beneath a strain gage showed up as an indicated tensile strain inasmuch as the Baldwin SR-4 type A-9 gages were not temperature compensated. Temperature calibration of the strain gage was performed by installing the gage on an unrestrained piece of 2014-T6 aluminum alloy and then heating the assembly slowly and uniformly in a furnace. Gage output was plotted against temperature rise and a linear calibration factor of 6.95 microinches per inch tensile strain per degree Fahrenheit temperature rise was established up to 180° F. For this temperature calibration, a three-wire gage hookup was used so that temperature changes in the lead wires would not affect the gage output.

Indicated strains obtained during the beam tests were corrected for temperature effects to give strains produced only by stress.

APPENDIX B

MATERIAL PROPERTIES

In order to calculate buckling and failure strengths for the beams reported herein, material properties were required for the appropriate temperatures, heating rates, and exposure times used in the beam tests. Material properties of these drawn square tubes of 2014-T6 aluminum alloy have been found previously to be quite uniform. The following properties were found to exist at room temperature both within any given cross section and throughout a series of tube sizes:

Property	Compression	Tension
0.2-percent-offset yield stress		
With grain, ksi	61.8	59.8
Cross grain, ksi	62.5	59.1
Young's modulus, ksi	10,700	10,500

The compression data are from reference 4 and the tension data are from an unpublished investigation. Spot checks of the material properties of the beams in this investigation indicated that these material properties were within the previously mentioned limits.

Experimental stress-strain curves were not available for the rapid-heating and/or rapid-loading conditions imposed on the beams. Tensile tests for the material heated rapidly under constant load were performed in a manner comparable to that described in reference 5. The tensile yield stresses obtained for a 0.2-percent-offset strain are shown in figure 9 for a temperature rate of 100° F per second. Similar curves were obtained for other values of offset strain. Tensile stress-strain curves at constant temperature were then obtained by cross-plotting the offset-strain data and adding a calculated elastic strain determined by using values of Young's modulus at elevated temperature given in reference 6. Compression stress-strain curves (fig. 10) were constructed similar in shape to the tensile curves but an allowance was made for the difference in compression and tensile yield stresses at any given temperature. Compressive yield stresses were estimated at elevated temperatures by assuming that the percentage reduction in yield stress at any temperature is the same for compression as for tension.

In the present report, the secant modulus is the only material property required from the constructed stress-strain curves. This material

property is relatively insensitive to small variations in the stress-strain curve for stress less than the yield stress. The tangent modulus or slope of the stress-strain curve, on the other hand, may be quite sensitive to small variations in the shape of the curve. The assumption was made in the construction of these stress-strain curves that yield stresses determined by rapid heating under constant load were the same as yield stresses determined by rapid loading under constant temperature. In order for this condition to exist, the effect of exposure to temperature must be comparable in the two cases and the strain rates in the two cases must be the same. Both of these requirements are difficult to evaluate and to control experimentally. For the beam tests reported herein, the total test time to failure was less than 10 seconds whether the beams were heated first and then loaded or loaded first and then heated.

APPENDIX C

METHODS OF ANALYSIS

Determination of Average Test Temperatures

For the uniformly heated square tubes, average beam temperatures were taken as the arithmetic average of all the thermocouple readings around the cross section, such as are shown by the dashed lines in figures 5 and 6. For the tests in which skin heating was used, average skin temperatures and average web temperatures, such as those shown by the dashed lines in figures 3 and 4, were computed by using graphical integration of the area under the portion of the temperature curve plotted for either the skin or the web, respectively.

Heating tests of both the 5.00-inch- and 7.50-inch-square tubes indicated reasonable repeatability of average beam, skin, and web temperatures, as shown in figure 11 for the 5.00-inch-square tubes. The average temperatures are plotted as a function of the peak temperature in the compression skin at the center of the loaded section. Thus in subsequent tests, instead of using 10 to 15 thermocouples in each specimen to determine temperature distributions, 3 thermocouples were used and were spaced 1 inch apart along the longitudinal center line of the compression skin. Peak temperatures in the test, as determined by the average from these 3 thermocouples, were used in figure 11 to read the average beam, skin, or web temperature for the 5.00-inch-square tubes. A similar figure was used for the 7.50-inch-square tubes.

A variation in temperature existed through the thickness of the heated tube walls. Calculations have indicated that, for the heating rate, peak temperature, and thickness of aluminum used in these experiments, a maximum temperature difference of 3 percent of peak temperature existed between the two surfaces of the heated wall. Inasmuch as the exact location of the thermocouple within the thickness of the material was uncertain and the possible error was small, measured temperatures at any point were taken to represent the average through the thickness at that point.

Experimental Buckling

Buckling is defined herein as the beginning of rapid growth of sinusoidal buckles in the compression skin of the beam, produced by the combination of bending moment and heating. The experimental determination of local skin buckling under these circumstances was sometimes quite difficult.

Buckling was determined from the test records when the indicated rate of web bending strains, as measured by wire strain gages, or the rate of beam deflections, as measured by transformer gages, showed a sudden change with respect to either moment or temperature. Web strains obtained in the tests in which skin heating was used generally showed a more pronounced change than the deflections. The method of determining buckling is based on the observation that the longitudinal compressive stiffness of a buckled plate in the elastic range may be reduced approximately 50 percent, the reduction depending upon edge conditions of the plate. (See, for example, ref. 7.) This reduction in longitudinal compression stiffness is even greater when buckling occurs at stresses above the proportional limit of the material. Reduction of the stiffness of the compression skin after buckling changes the beam into an unsymmetrical structure. Continued symmetrical heating of an unsymmetrical beam will produce beam bending as the tension skin expands more than the buckled compression skin. Thus, with heating, the beam deflections grow at a faster rate after buckling than before buckling, and strain rates change at the transition from symmetrical to unsymmetrical beam behavior.

Theoretical Buckling

Buckling at constant temperature.- The theoretical buckling stress for the skin of a square-tube beam loaded in bending is given by the following plate-buckling equation:

$$\sigma_{cr} = \frac{-k\pi^2\eta E}{12\left(1 - \mu^2\right)}\left(\frac{t}{b}\right)^2 \tag{C1}$$

A stability analysis of a uniformly heated plate structure which takes into account the rotational restraint supplied to the side edges of the skin by the webs of the beam, such as in reference 8, yields a value for the buckling coefficient k of 5.32 which is independent of material or temperature.

Buckling due to thermal stress.- For the skin heated beams, buckling can occur as a result of the thermal stresses which develop because of the temperature difference between the skins and webs. These thermal stresses can be evaluated by satisfying the conditions of equilibrium and continuity. The total longitudinal strain at any point in the cross section can be expressed as

$$\epsilon_t = \frac{\sigma}{E_S} + \alpha(T - T_O) \tag{C2}$$

from which

$$\sigma = E_S\left[\epsilon_t - \alpha(T - T_o)\right] \tag{C3}$$

Compressive stresses and strains were taken as negative and tensile stresses and strains were taken as positive. Because thermal stresses are self-equilibrating, equilibrium of forces requires that

$$\int \sigma \, dA = 0 \tag{C4}$$

Symmetrical heating of a symmetrical structure produces no bending deformation; therefore, the total strain must be a constant at every point,

$$\epsilon_t = \text{Constant} \tag{C5}$$

Algebraic solution of equation (C3) for the thermal stress, subject to the conditions of equations (C4) and (C5), can be obtained only if the temperature distribution, the secant modulus, and the coefficient of expansion are expressed as known functions of the cross section and strain. However, numerical solutions can be obtained after subdividing the structure into a finite number of incremental areas for each of which an average temperature can be obtained, and then values of E_S and α can be obtained for these temperatures and strains. When this method and the temperature distribution given in figure 3 for the skin heating of a 5-inch-square tube were used, a numerical solution for the thermal-stress distribution was made by dividing the quadrant of the beam into 16 equal increments. Values of E_S were obtained from figure 10 and values of α were obtained from reference 3. The resulting thermal-stress distribution is plotted in figure 12 as the solid curve which was drawn through the 16 incremental points.

If the temperature distribution in figure 3 is idealized as a constant temperature in the skin equal to the average value $\overline{T}_S$ and a constant temperature in the web equal to $\overline{T}_W$, a direct solution for thermal stress is obtained.

Equations (C3) and (C4) become

$$\sigma_S = E_S\left[\epsilon_t - \alpha_S\left(\overline{T}_S - T_o\right)\right] \tag{C6a}$$

$$\sigma_W = E_W\left[\epsilon_t - \alpha_W\left(\overline{T}_W - T_o\right)\right] \tag{C6b}$$

$$\int \sigma \, dA = \sigma_S A_S + \sigma_W A_W = 0 \tag{C7}$$

Eliminating the constant strain ϵ_t and solving for the thermal stress in the skin give

$$\sigma_S = \frac{-\alpha E_S\left(\overline{T}_S - \overline{T}_W\right)}{1 + \frac{E_S A_S}{E_W A_W}} \tag{C8}$$

This expression is equally valid for plastic or elastic stresses. Secant moduli used for plastic stresses must be evaluated at stresses related by equation (C7). The coefficient of thermal expansion α is evaluated over the range of temperatures between $\overline{T}_S$ and $\overline{T}_W$.

The thermal-stress distribution given by equations (C7) and (C8) and corresponding to the idealized constant-skin, constant-web temperature distribution is shown in figure 12 by the dashed line. The web and skin loads are approximately the same as those given by the analysis which uses the more precise temperature distribution.

If the skin heating continues until a sufficiently large temperature difference occurs between skins and webs, the thermal stress developed causes local buckling of the skin without any external load. The magnitude of the stress required to buckle the skin thermally can be determined from equation (C1). However, the value of k must be determined for suitable boundary conditions.

For the assumed rectangular temperature distribution in the square tube, the skin can be assumed to be a long plate uniformly compressed with the side edges supported by long plates uniformly stressed in tension by the same magnitude of stress. A stability analysis of such a

structure was made by following the procedure of reference 9. Buckling occurs when the sum of the stiffnesses of the compressed skin and the tensile-loaded web is zero. The buckle wave length in the skin and in the web must be the same and the magnitude of the stresses must be the same for a square tube with equal skin and web thicknesses. Stiffnesses for the compressed plate are tabulated in reference 10 as a function of buckle wave length and stress. Stiffnesses for the web plate loaded in tension were calculated with the use of equation (A48) of reference 9. When the foregoing analysis was made, the increased stiffness of the tensile plates resulted in a value of $k = 5.59$ for the skin, if Young's modulus was assumed to be the same for the skin and the web. Because the skin is at a higher temperature than the web, Young's modulus for the skin is less than that for the web and results in a greater difference in stiffnesses and a slightly higher value of k, depending upon the modulus change. Calculations based on this analysis give the variation of k shown in figure 13 for thermal buckling of the skin of a square tube of 2014-T6 aluminum alloy at various skin temperatures when the web temperature is as shown in figure 11.

The thermal-buckling solution is obtained by equating equation (C1) and equation (C8), assuming a value for k slightly greater than 5.59, computing the resulting temperature difference $\left(\overline{T}_S - T_W\right)$, reading a better value of k from figure 13 at $\overline{T}_S$, and then repeating the process until k and $\overline{T}_S$ are consistent with one another.

Buckling due to combinations of bending and thermal stress.- For buckling under a combination of bending and skin heating, the value of the skin buckling coefficient k should be between the pure bending end point of 5.32 and the thermal end point which will be greater than 5.59. If a linear variation in k with skin temperature between the end-point values is assumed, the correct value to use for combined bending and thermal buckling is given by the following equation:

$$k = 5.32 + \left(\frac{\overline{T}_S - 80}{\overline{T}_{S,cr} - 80}\right)\left(k_{thermal} - 5.32\right) \qquad (C9)$$

Buckling will occur when the combination of skin stress due to bending and skin stress due to skin heating is equal to the buckling stress calculated by using k from equation (C9). Thus at any given skin temperature, the buckling stress and the thermal stress can be determined, and the difference must be supplied by bending load stress in order to produce skin buckling. Then

$$\sigma_B = \sigma_{cr} + \frac{\alpha E_S\left(\overline{T}_S - \overline{T}_W\right)}{1 + \frac{E_S A_S}{E_W A_W}} \tag{C10}$$

which is given as equation (2) in the section entitled "Results and Discussion."

Failure

The experimentally observed results at failure are discussed in the section entitled "Results and Discussion." An expression for the moment carried at failure can be obtained by summing the moments carried by the skins and the webs. The moment calculation is based on stress distributions developed as follows.

The average stress carried by a compressed plate at failure was expressed in reference 11 as

$$\sigma_S = -1.60\sqrt{E_S\sigma_{cy}}\left(\frac{t_S}{b_S}\right) \tag{C11}$$

The coefficient 1.60 contains the term $\sqrt{k}$ and was evaluated from a comparison with plate tests in compression in which most of the plates had a buckling coefficient of about 4. For the bending tests in which uniformly heated beams were used, the buckling coefficient is 5.32 and some modification of the expression for σ_S is necessary; thus assume that

$$\sigma_S = -1.60\sqrt{\frac{k}{4.00}}\sqrt{E_S\sigma_{cy}}\left(\frac{t_S}{b_S}\right) \tag{C12}$$

Therefore, taking moments about the tension skin gives for the skin at failure

$$M_S = 1.84\sqrt{E_S\sigma_{cy}}t_S^{\,2}b_W \tag{C13}$$

Examination of the strains in several integral-web beams indicated that the compression edge of the web reached the yield stress prior to failure of the beams. Even though a neutral axis shift occurred because of the buckling of the skin, an expression for the moment carried by the web, which agreed with the results of the tests at room temperature of this paper as well as with previous test results, was found to be

$$M_W = \frac{1}{5} \sigma_{cy} b_W^2 t_W \qquad (C14)$$

This moment equation assumes that the neutral axis remains at the center of the web and the stress distribution is partially plastic, with the extreme fiber stress equal to the yield stress.

When equations (C13) and (C14) are combined, the failure moment for the beam can be written as

$$M_f = 1.84 \sqrt{E_S \sigma_{cy}} t_S^2 b_W + 0.400 \sigma_{cy} b_W^2 t_W \qquad (C15)$$

The secant modulus for the skin is evaluated at a stress given by equation (C12). Substituting the actual beam dimensions into these equations and using material properties at the appropriate temperatures permit the curves of failure moment shown in figure 8 to be calculated.

REFERENCES

1. Pride, Richard A.: An Investigation of the Effects of Rapid Skin Heating on Box Beams Loaded in Bending. NACA RM L55B03, 1955.

2. Pride, Richard A., Hall, John B., Jr., and Anderson, Melvin S.: Effects of Rapid Heating on Strength of Airframe Components. NACA TN 4051, 1957.

3. Anon.: Alcoa Aluminum and Its Alloys. Aluminum Co. of America, 1950.

4. Pride, Richard A., and Heimerl, George J.: Plastic Buckling of Simply Supported Compressed Plates. NACA TN 1817, 1949.

5. Heimerl, George J., and Inge, John E.: Tensile Properties of 7075-T6 and 2024-T3 Aluminum-Alloy Sheet Heated at Uniform Temperature Rates Under Constant Load. NACA TN 3462, 1955.

6. Anon.: Strength of Metal Aircraft Elements. ANC-5 Bull., Rev. ed., Depts. of Air Force, Navy, and Commerce, Mar. 1955.

7. Hu, Pai C., Lundquist, Eugene E., and Batdorf, S. B.: Effect of Small Deviations From Flatness on Effective Width and Buckling of Plates in Compression. NACA TN 1124, 1946.

8. Schuette, Evan H., and McCulloch, James C.: Charts for the Minimum-Weight Design of Multiweb Wings in Bending. NACA TN 1323, 1947.

9. Lundquist, Eugene E., Stowell, Elbridge Z., and Schuette, Evan H.: Principles of Moment Distribution Applied to Stability of Structures Composed of Bars or Plates. NACA Rep. 809, 1945. (Supersedes NACA WR L-326.)

10. Kroll, W. D.: Tables of Stiffness and Carry-Over Factor for Flat Rectangular Plates Under Compression. NACA WR L-398, 1943. (Formerly NACA ARR 3K27.)

11. Anderson, Roger A., and Anderson, Melvin S.: Correlation of Crippling Strength of Plate Structures With Material Properties. NACA TN 3600, 1956.

TABLE I.- EXPERIMENTAL COMBINATIONS OF BENDING MOMENT AND TEMPERATURE THAT PRODUCE BUCKLING AND FAILURE

[Square-tube beams of 2014-T6 aluminum alloy; temperature rate, 100° F per second]

Beam	Sequence of loading and heating	Buckling			Failure		
		Moment, in-kips	$\bar{T}_S$, °F	$\bar{T}_W$, °F	Moment, in-kips	$\bar{T}_S$, °F	$\bar{T}_W$, °F
Outside width, 5.00 in.; wall thickness, 0.154 in.							
1	Room temperature	245.8	80	80	268.6	80	80
2	Uniformly heated, then loaded	178.6	463	463	187.5	463	463
3	Uniformly heated, then loaded	213.4	355	355	227.8	355	355
4	Loaded, then uniformly heated	188.0	455	455	188.0	474	474
5	Loaded, then uniformly heated	230.6	304	304	230.6	380	380
6	Loaded, then skin heated	179.2	276	98	179.2	579	151
7	Loaded, then skin heated	214.4	208	89	214.4	469	132
8	Loaded, then skin heated	244.8	101	82	244.8	307	102
9	Skin heated, then loaded	31.0	587	169	180.0	577	185
10	Skin heated, then loaded	85.0	495	158	198.0	495	158
11	Skin heated, then loaded	143.1	370	121	222.0	364	125
12	Skin heated, then loaded	172.1	252	106	234.4	250	111
Outside width, 7.50 in.; wall thickness, 0.152 in.							
13	Room temperature	234.0	80	80	471.0	80	80
14	Uniformly heated, then loaded	205.4	623	623	268.6	623	623
15	Uniformly heated, then loaded	(a)	477	477	395.2	477	477
16	Uniformly heated, then loaded	241.0	320	320	464.0	316	316
17	Loaded, then uniformly heated	238.8	80	80	280.0	610	610
18	Loaded, then uniformly heated	293.0	80	80	402.0	423	423
19	Loaded, then skin heated	220.0	172	87	220.0	(a)	(a)
20	Loaded, then skin heated	251.0	80	80	346.8	529	137
21	Loaded, then skin heated	238.2	80	80	404.0	405	119
22	Skin heated, then loaded	[b]0.0	393	108	335.0	600	128
23	Skin heated, then loaded	[b]0.0	394	108	351.8	576	156
24	Skin heated, then loaded	[b]0.0	389	122	390.0	446	129
25	Skin heated, then loaded	89.2	309	112	443.0	320	123

[a]Not determined because of equipment malfunction.

[b]Beam buckled during heating prior to loading.

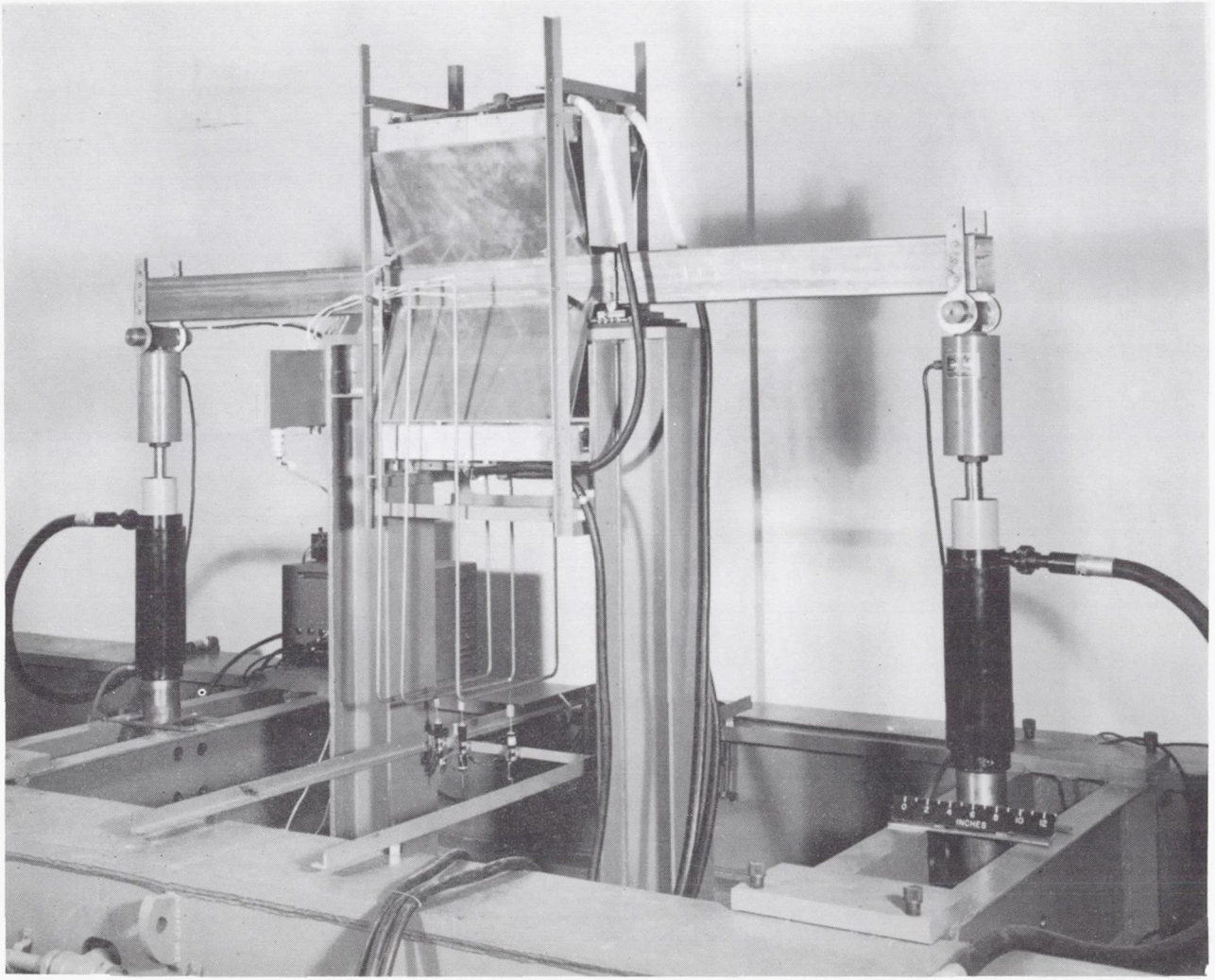

L-91930

Figure 1.- Test setup for applying bending loads and rapid heating on square-tube beams.

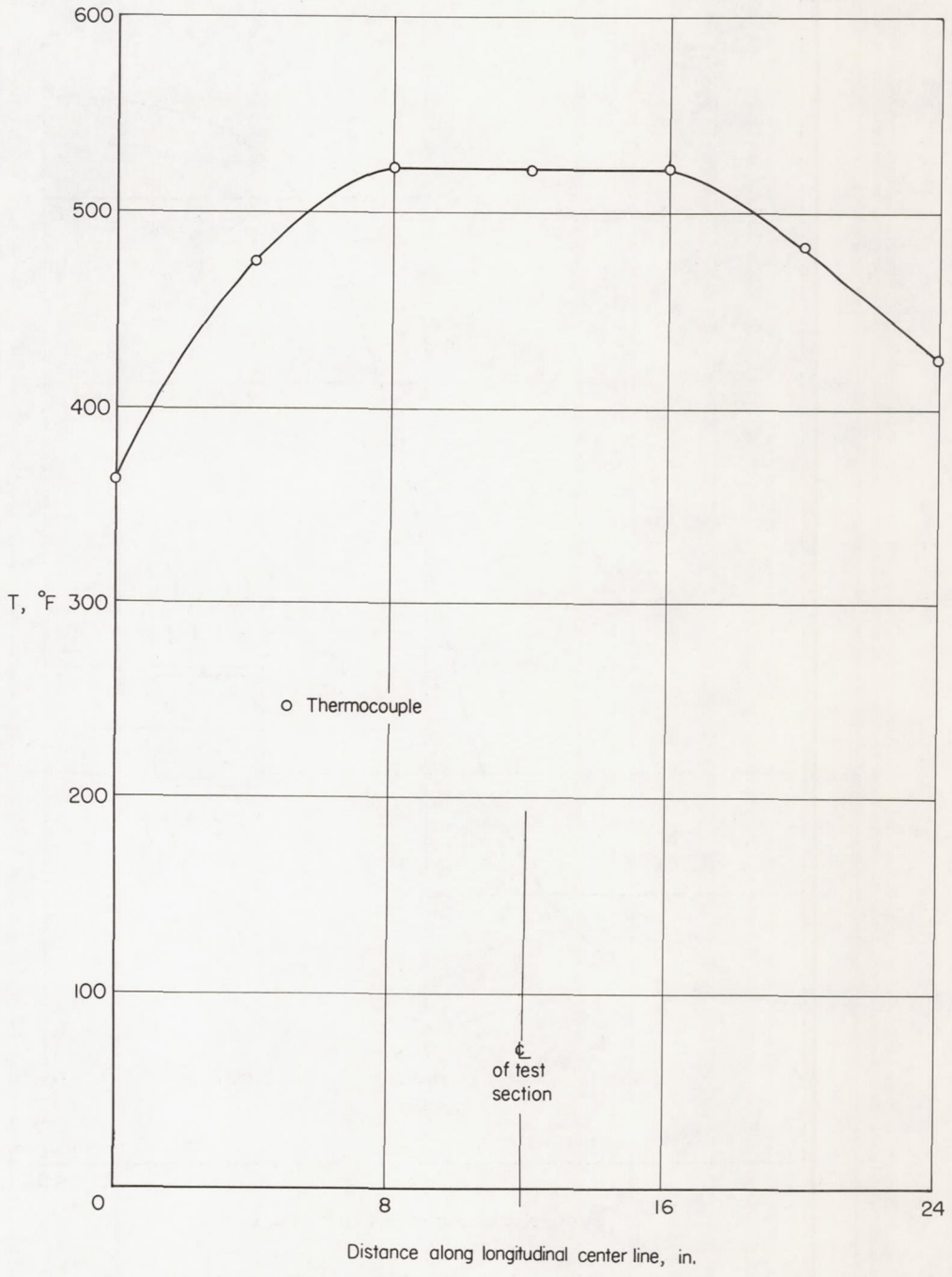

Figure 2.- Typical longitudinal temperature distribution for compression skin of square-tube beams made of 2014-T6 aluminum alloy and heated at a temperature rate of 100° F per second.

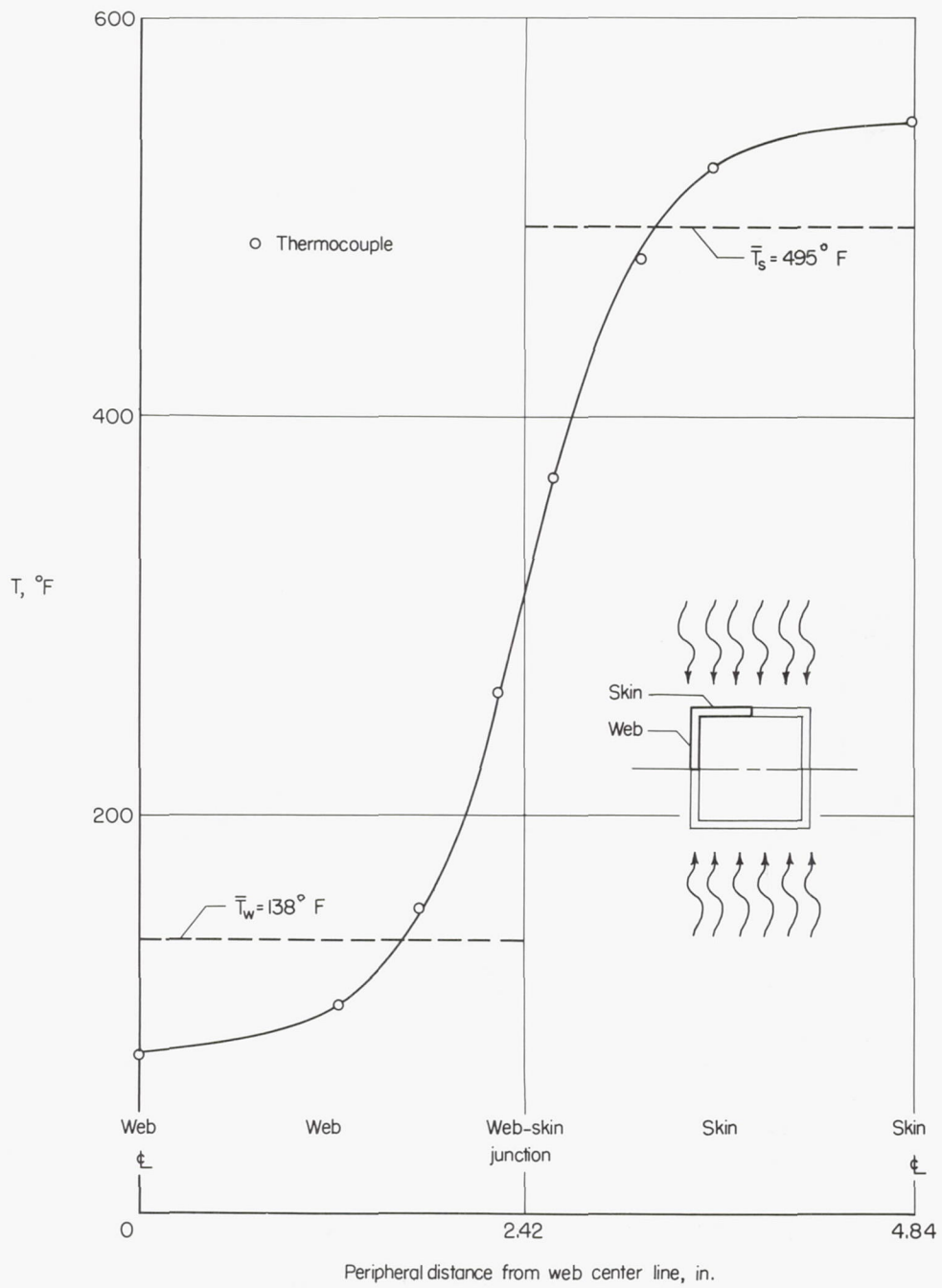

Figure 3.- Typical cross-sectional temperature distribution for 5.00-inch-square-tube beams made of 2014-T6 aluminum alloy and skin heated at a temperature rate of 100° F per second.

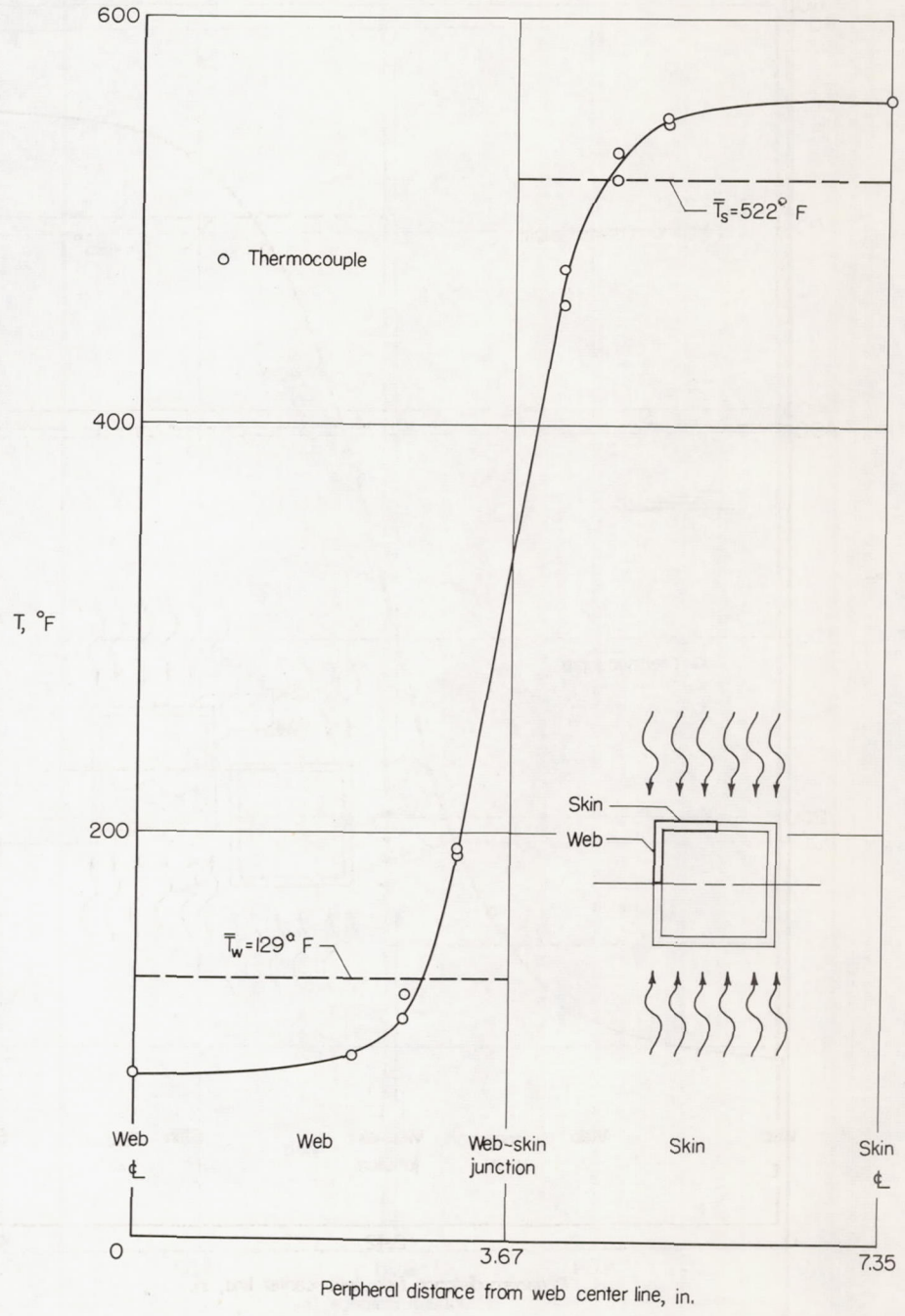

Figure 4.- Typical cross-sectional temperature distribution for 7.50-inch-square-tube beams made of 2014-T6 aluminum alloy and skin heated at a temperature rate of 100° F per second.

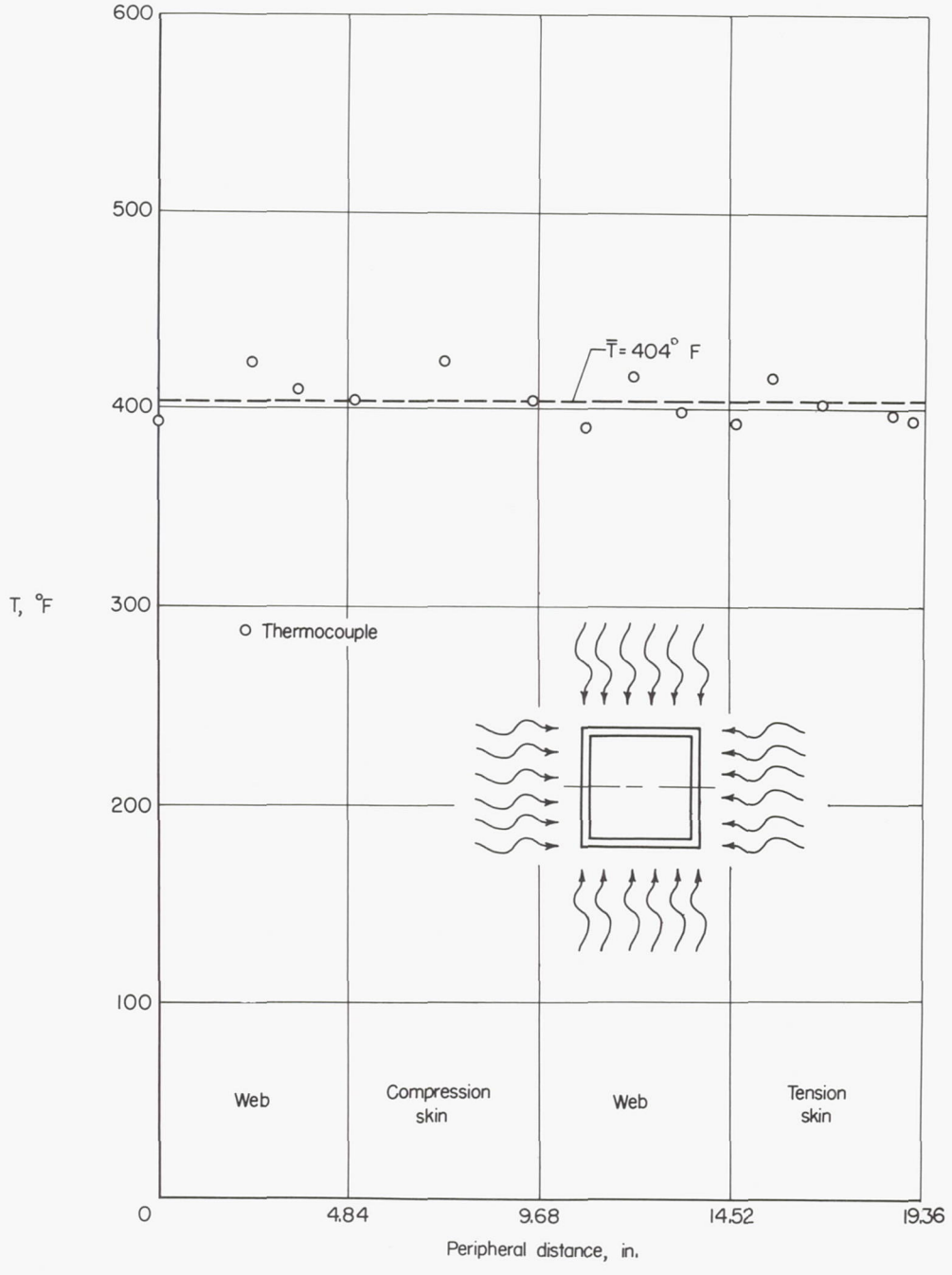

Figure 5.- Typical cross-sectional temperature distribution for 5.00-inch-square-tube beams made of 2014-T6 aluminum alloy and uniformly heated at a temperature rate of 100° F per second.

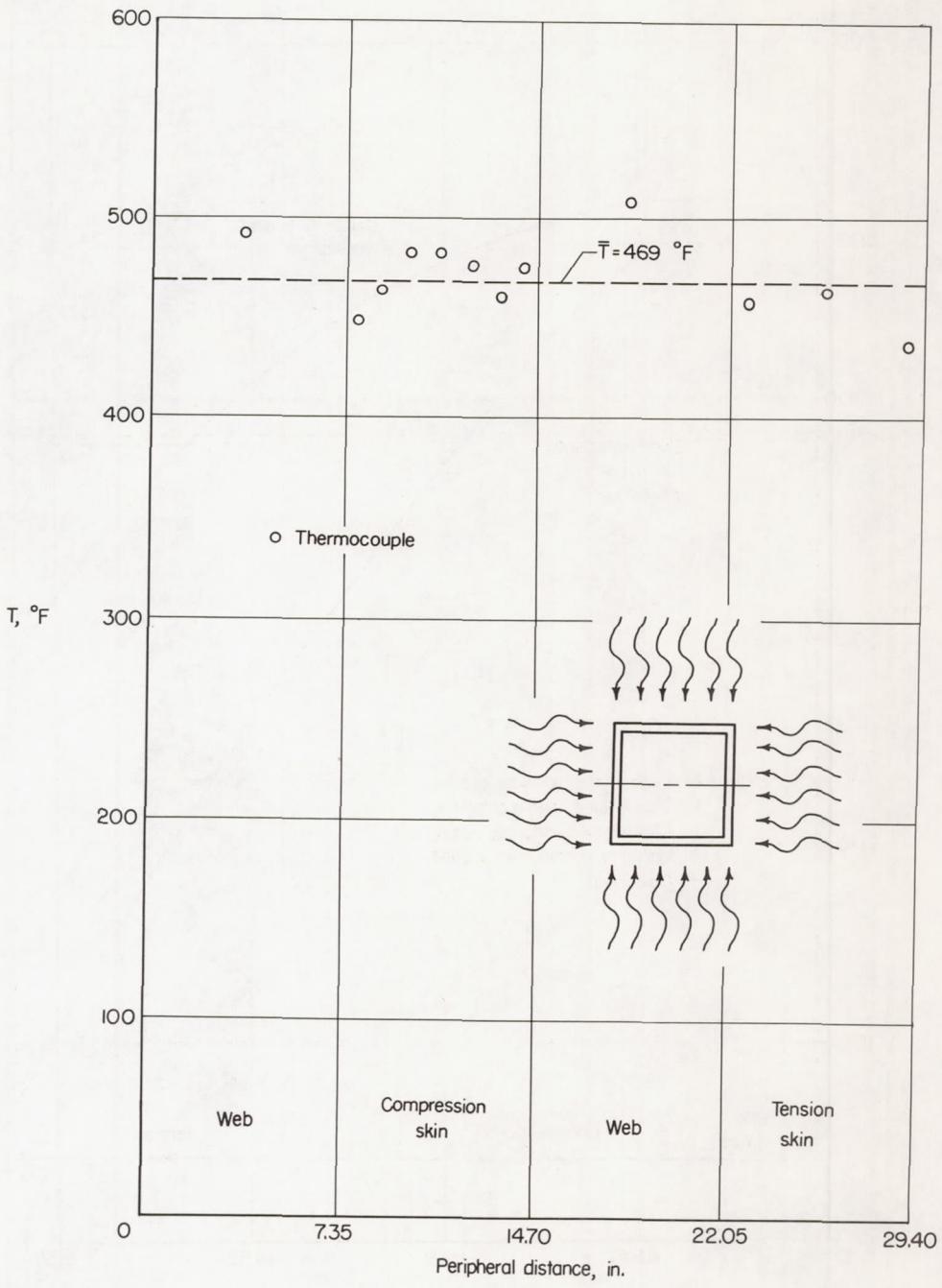

Figure 6.- Typical cross-sectional temperature distribution for 7.50-inch-square-tube beams made of 2014-T6 aluminum alloy and uniformly heated at a temperature rate of 100° F per second.

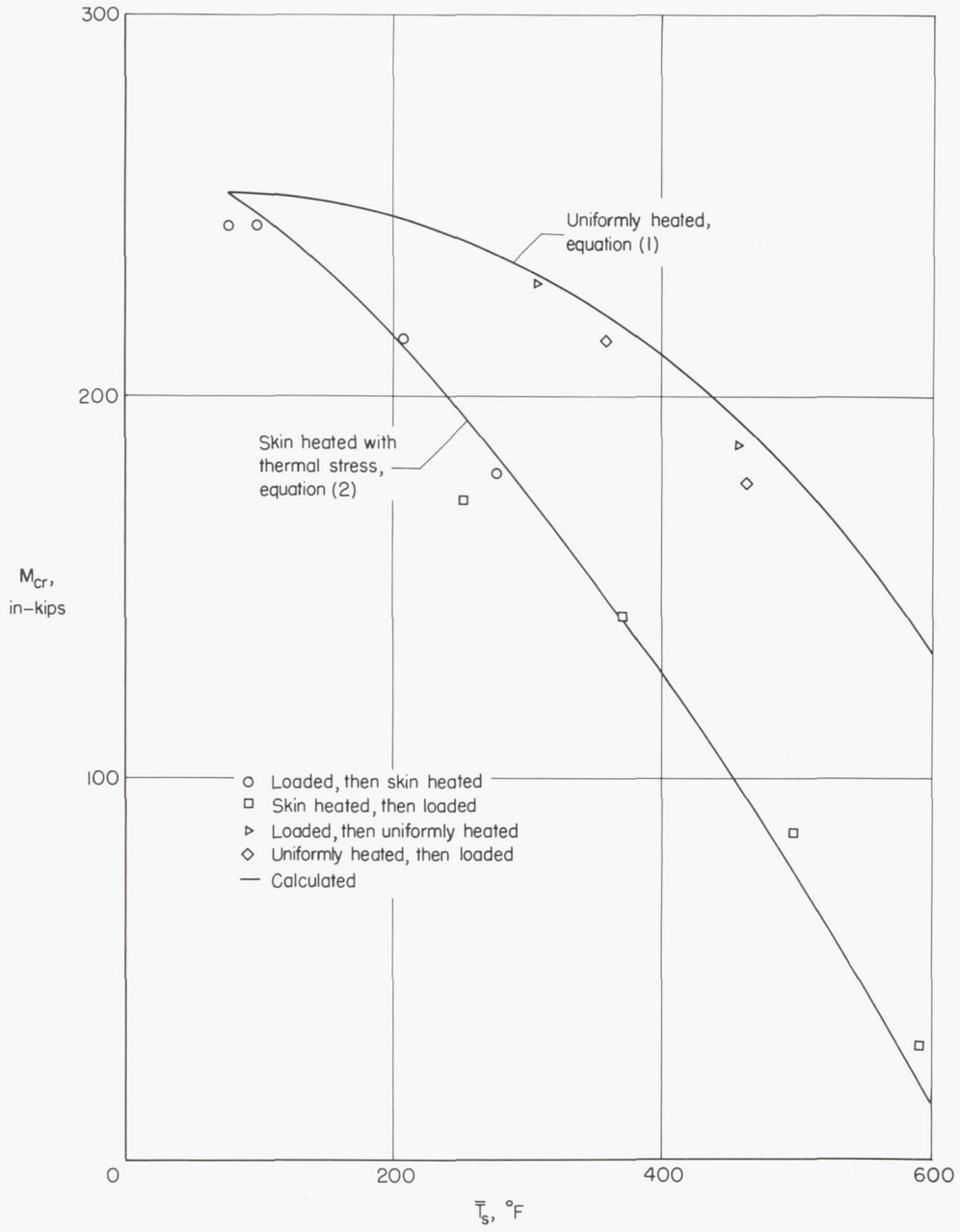

(a) The 5.00-inch-square tubes; $\frac{b}{t} = 31$.

Figure 7.- Effect of transient heating on the buckling strength of square-tube beams made of 2014-T6 aluminum alloy. Temperature rate, 100° F per second.

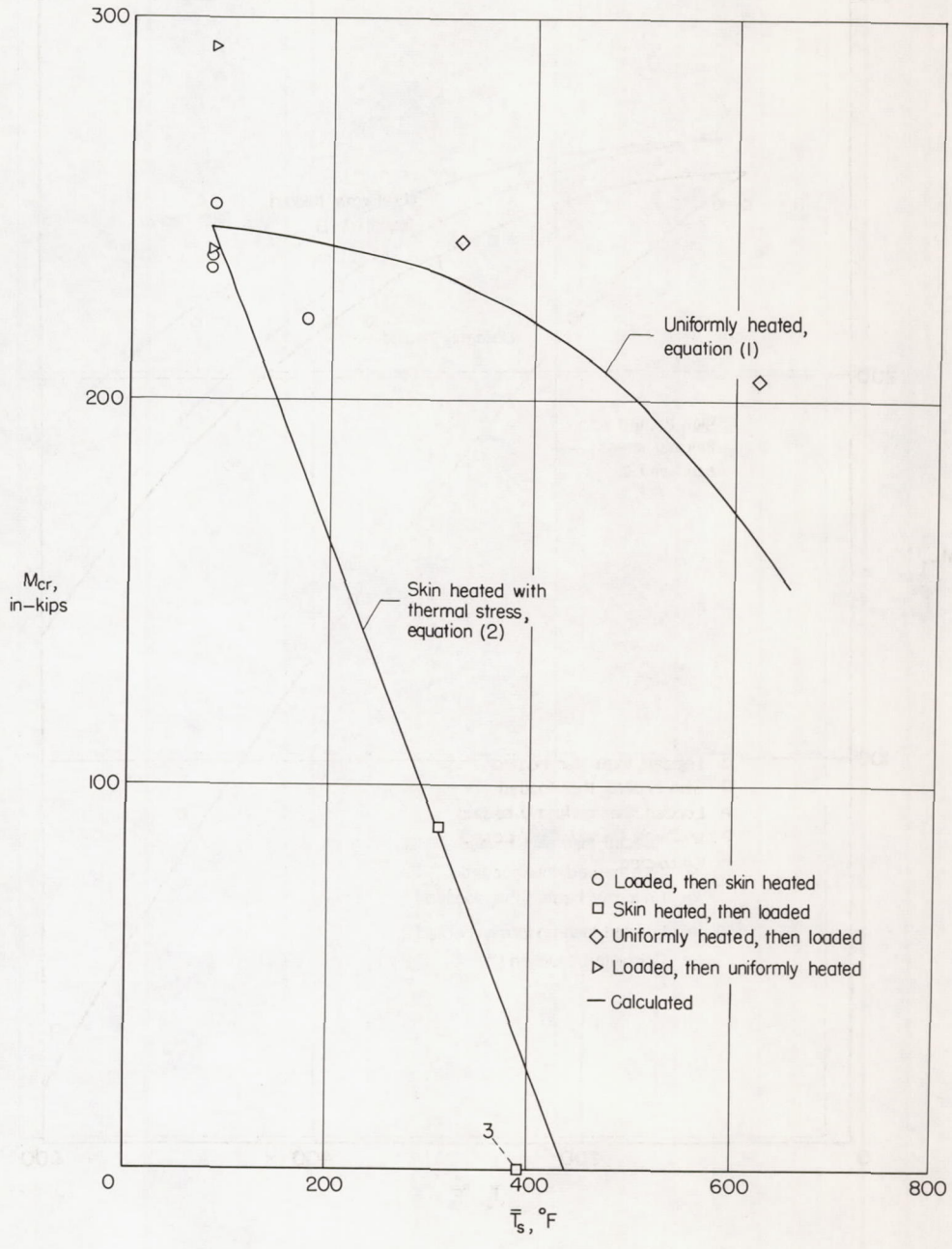

(b) The 7.50-inch-square tubes; $\frac{b}{t} = 48$.

Figure 7.- Concluded.

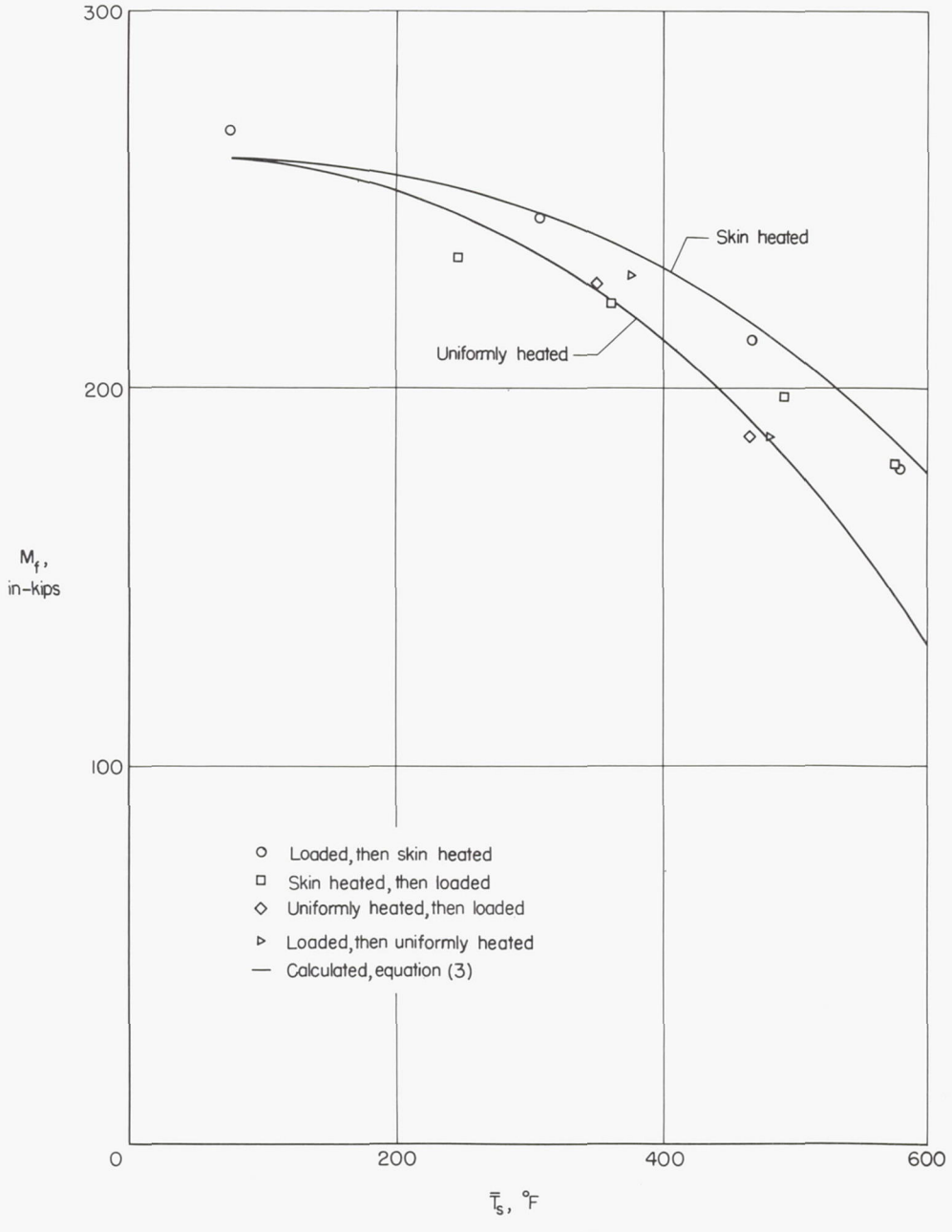

(a) The 5.00-inch-square tubes; $\frac{b}{t} = 31$.

Figure 8.- Effect of transient heating on the maximum strength of square-tube beams made of 2014-T6 aluminum alloy. Temperature rate, 100° F per second.

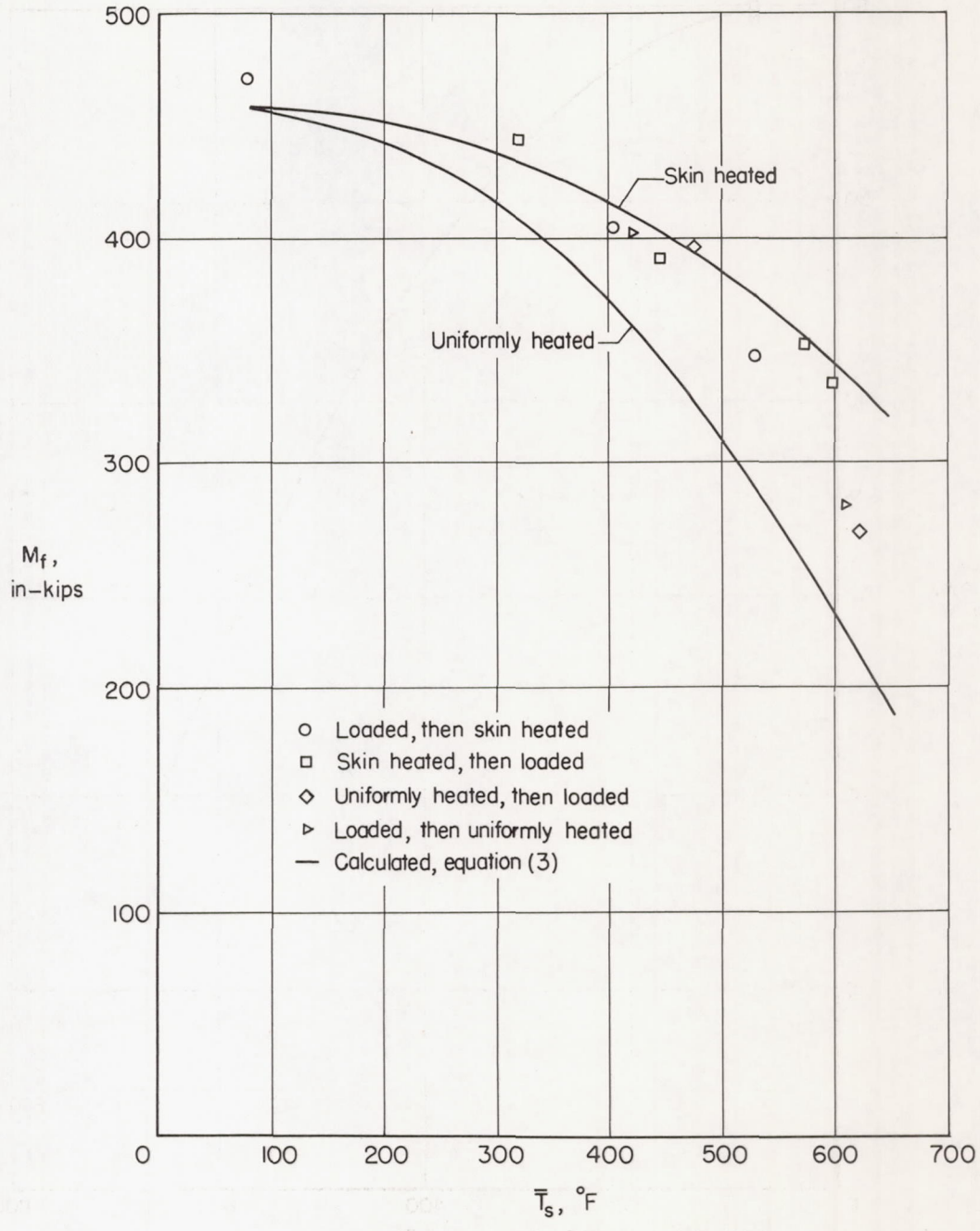

(b) The 7.50-inch-square tubes; $\frac{b}{t} = 48$.

Figure 8.- Concluded.

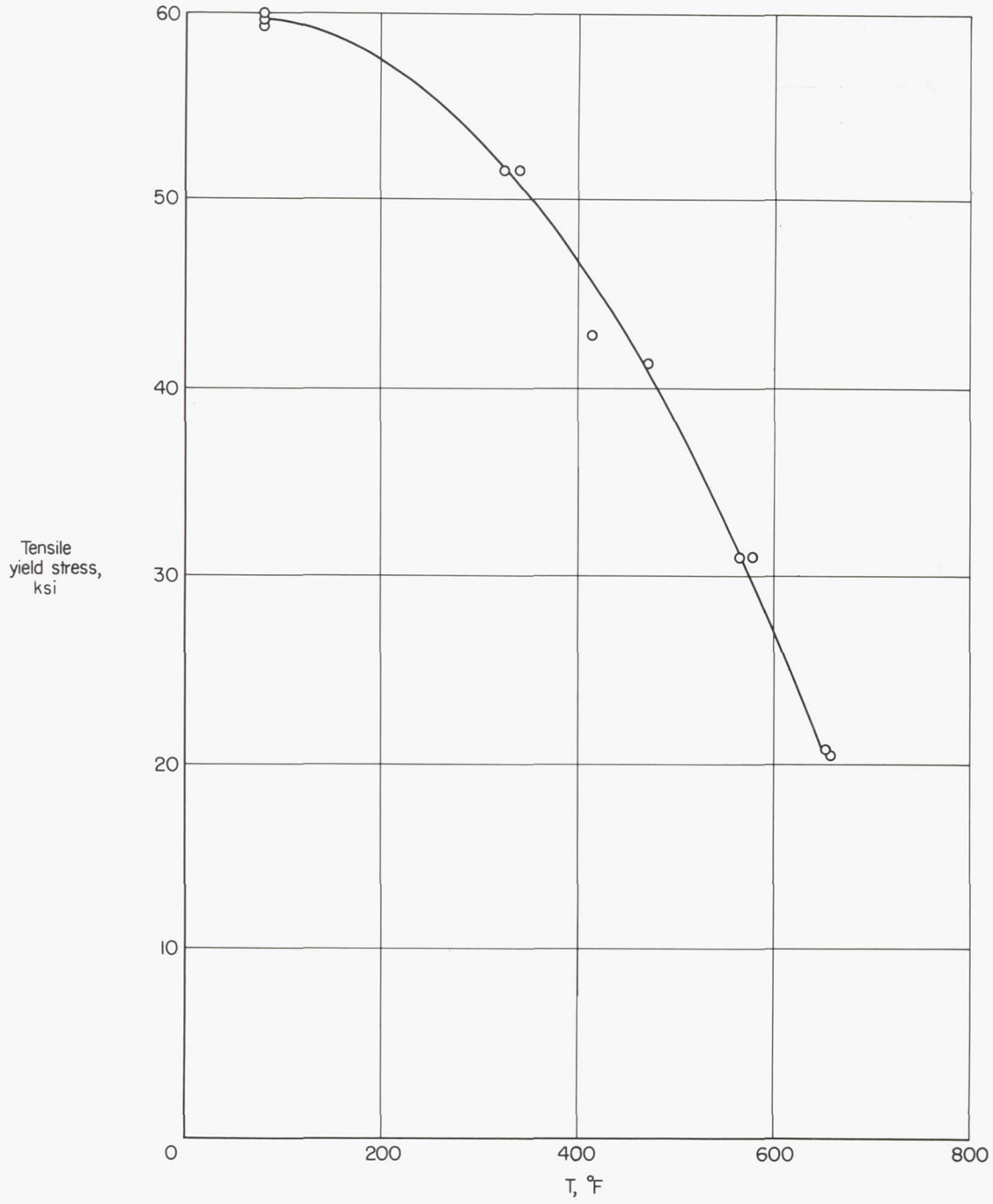

Figure 9.- Variation of tensile yield stress with temperature for 2014-T6 aluminum alloy heated at a temperature rate of 100° F per second.

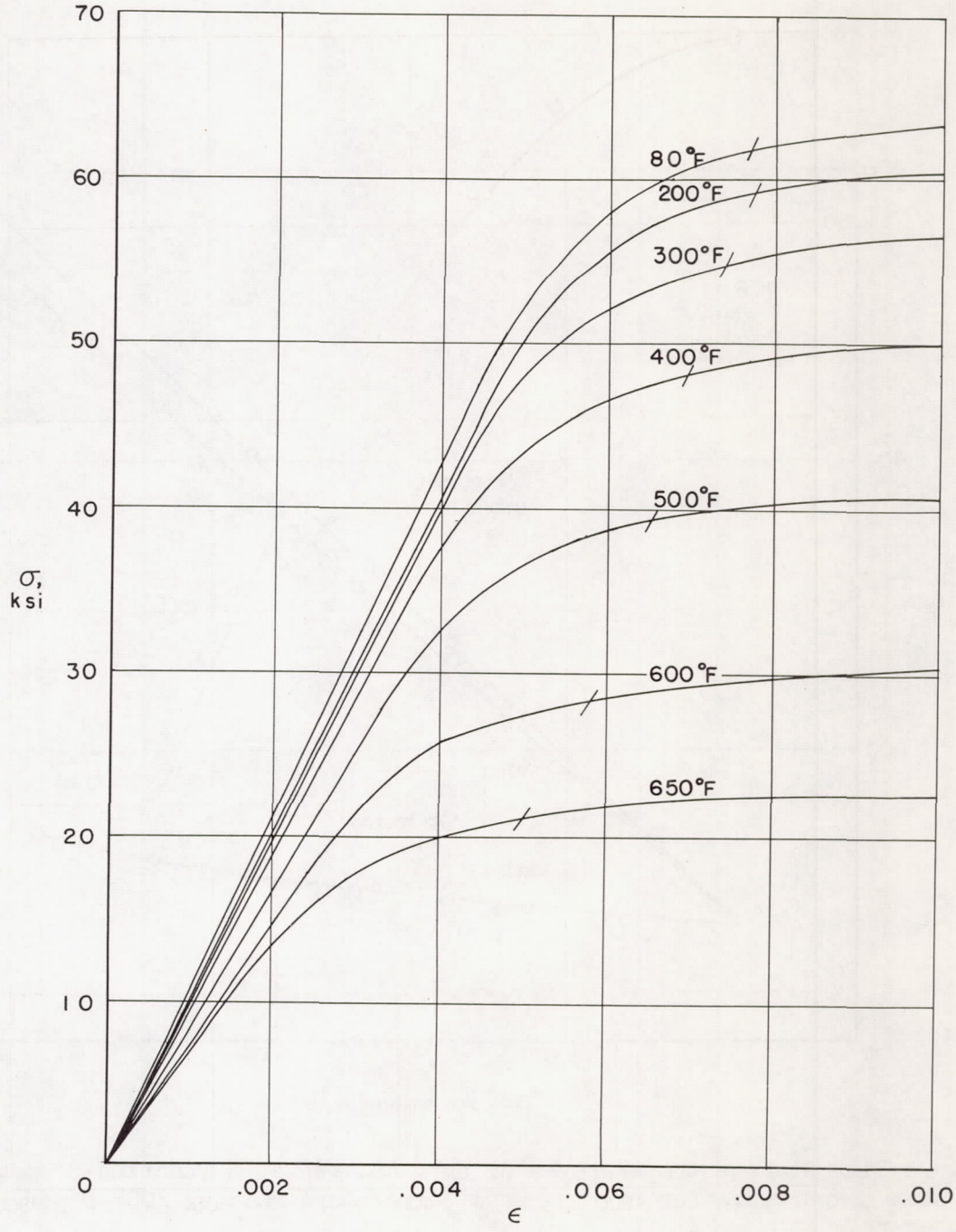

Figure 10.- Constructed compression stress-strain curves taken to be representative of 2014-T6 aluminum alloy when heated at a temperature rate of 100° F per second.

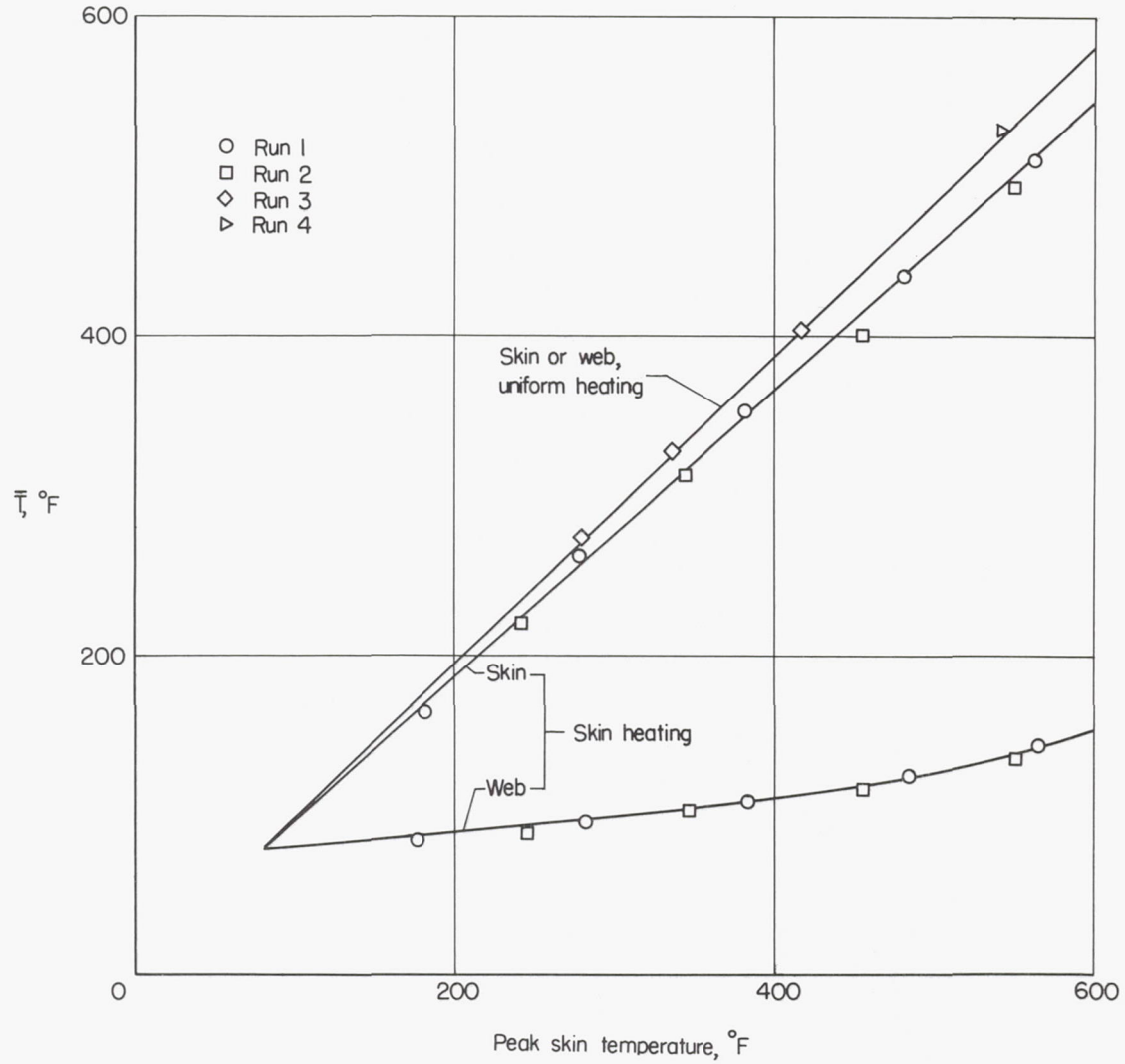

Figure 11.- Average temperatures of skin and web as a function of peak skin temperature for heating at a temperature rate of 100° F per second.

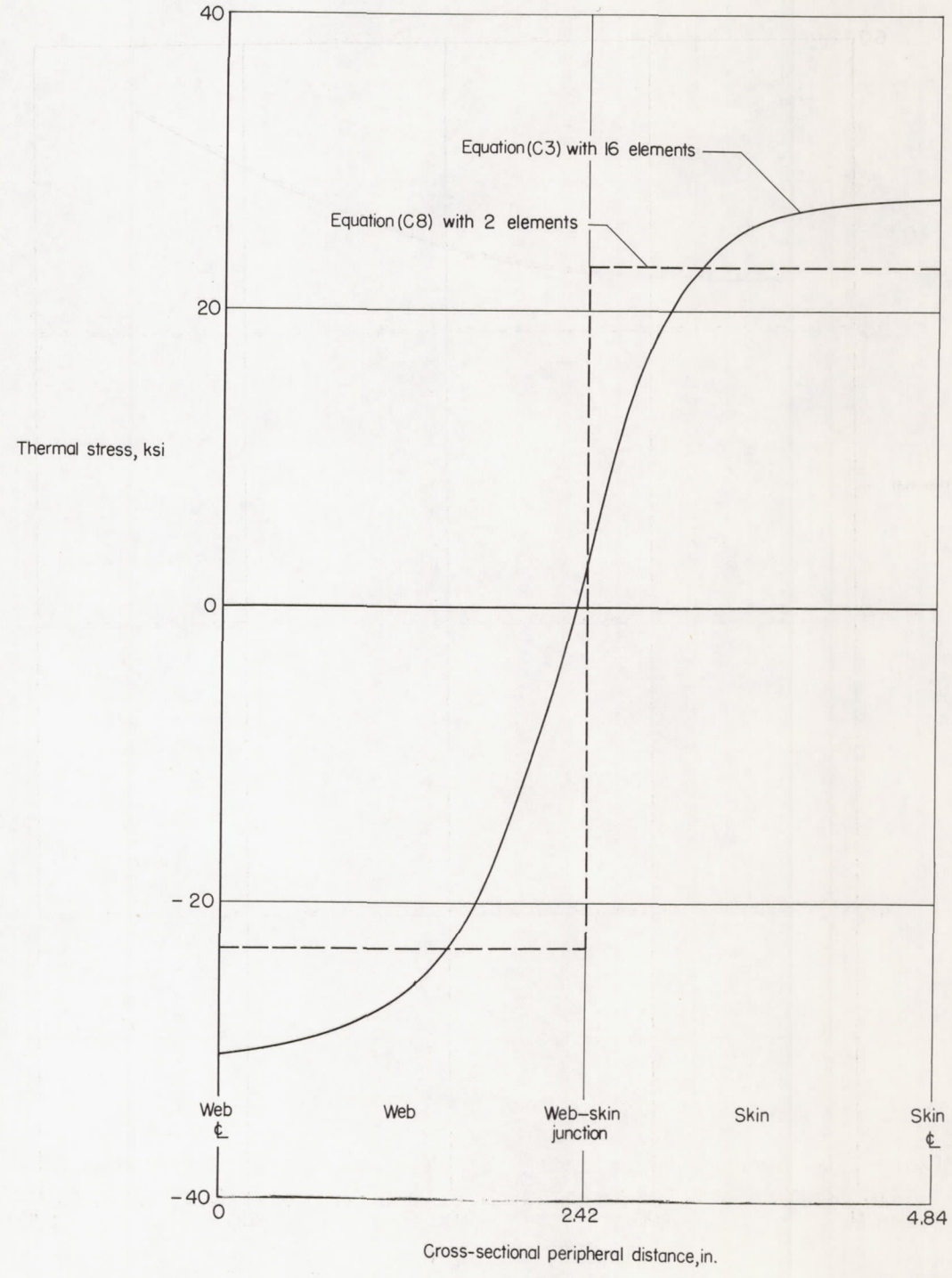

Figure 12.- Calculated thermal-stress distribution in one quadrant for a 5.00-inch-square tube subjected to skin heating.

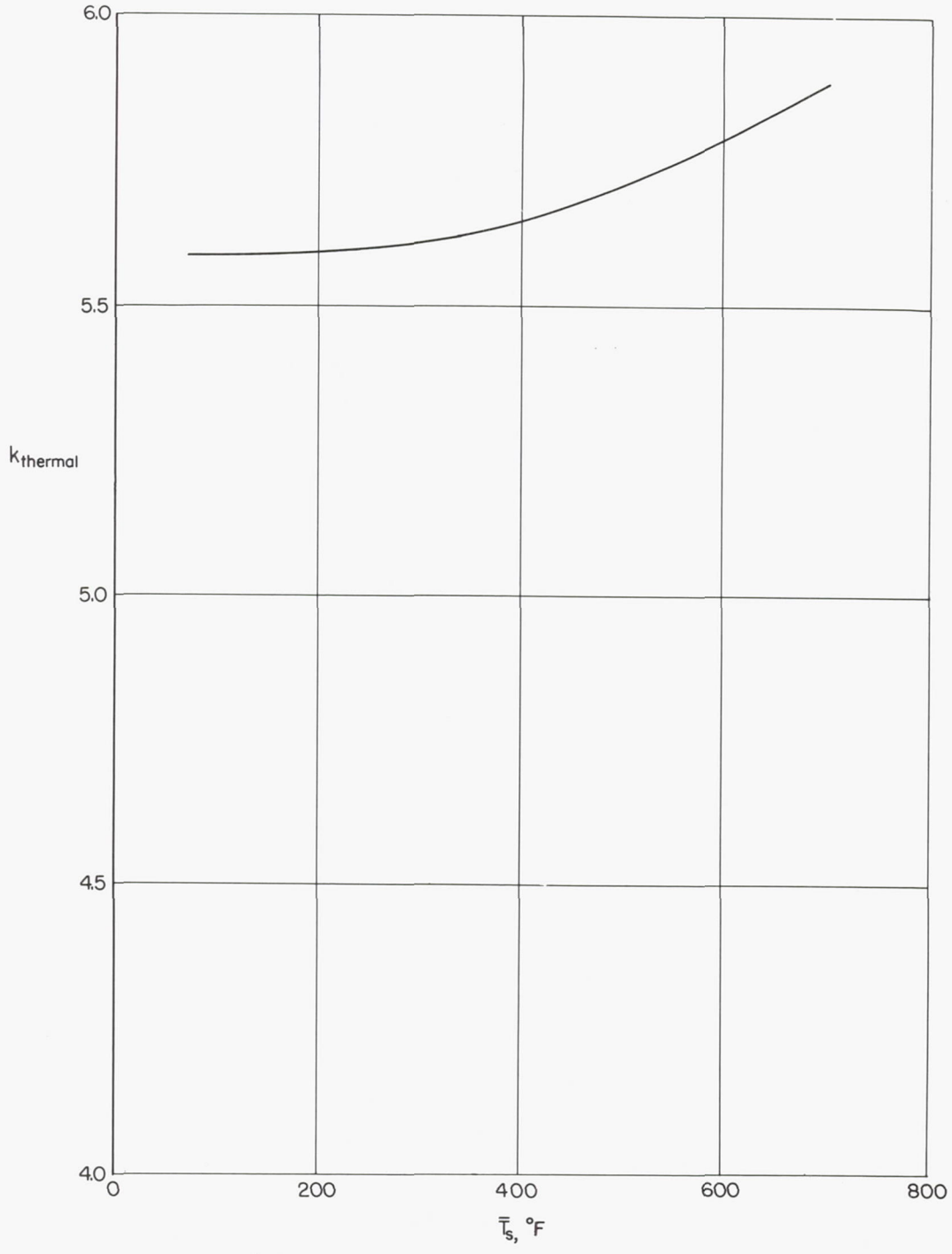

Figure 13.- Variation of skin buckling coefficient with temperature for thermal buckling of a square tube of 2014-T6 aluminum alloy.